SGP-TR-93-23

PROCEEDINGS
ELEVENTH WORKSHOP
GEOTHERMAL RESERVOIR ENGINEERING

January 21-23, 1986

Henry J. Ramey, Jr., Paul Kruger, Frank G. Miller,
Roland N. Horne, William E. Brigham,
and John R. Counsil
Stanford Geothermal Program
Workshop Report SGP-TR-84*

*Sponsored by the Geothermal and Hydropower Technologies Division of the U.S. Department of Energy, Stanford-DOE Contract No. DE-AS03-80SF11459 and Contract No. DE-AS07-84ID12529

DISCLAIMER

PROCEEDINGS, Eleventh Workshop on Geothermal Reservoir Engineering
Stanford University, Stanford, California, January 21-23, 1986
SGP-TR-93

Modeling Studies of Cold Water Injection into Fluid-Depleted, Vapor-Dominated Geothermal Reservoirs

C. Calore, K. Pruess**, and R. Celati**

*International Institute for Geothermal Research
Pisa, Italy

**Earth Sciences Division
University of California
Lawrence Berkeley Laboratory
Berkeley, California 94720

INTRODUCTION

Reinjection experiments in the strongly fluid-depleted reservoir of Larderello have revealed the possibility of increasing production rates and overall heat extraction by injection into high permeability, low pressure zones of the reservoir (Giovannoni et al., 1981; Cappetti et al., 1982; Bertrami et al., 1985). A large fraction (over 80%) of the injected water was recovered as steam in the most favorable area and, despite the short distance between injection and producing wells (the minimum distance being about 150 m), no significant temperature change has been observed in the latter, after 3 years of injection at a rate ranging from 10 to 50 kg/s (Bertrami et al., 1985).

The physical processes involved in cold water injection into a "superheated" fractured reservoir are not yet fully understood, and this insufficient knowledge of the fundamental mechanisms limits the possibility of forecasting future reservoir behavior and optimizing the heat extraction process. Numerical simulation can be a very effective tool in the study of the complex phenomena involved, allowing a rapid examination of different situations and conditions, a systematic investigation of the effects of various parameters on reservoir performance, and some insight into long term behavior. We have performed simulation experiments on simple one-dimensional, porous and fractured reservoir models in order to study the migration of injected water, thermodynamic conditions in the boiling zone, heat extraction, and vapor generation. A two-dimensional radial porous medium model, with some characteristics typical of the high productivity zones of Larderello, has also been applied for studying the evolution of the shape and the thermodynamic conditions of the injection plume in the presence of gravity, reservoir heterogeneities and anisotropy.

The MULKOM code was used for the simulations (Pruess, 1983).

One-dimensional, porous medium column

For our first simple case of injection of cold water into a "superheated" reservoir we consider a one-dimensional porous column initially at 240 °C and 6 bars. Water at 30 °C is injected at one end of the column and the other end is maintained at a constant pressure of 6 bars; gravity is ignored. The parameters of the system simulated are shown in Table I.

A sharp boiling front develops and advances through the column (Fig. 1). Temperature, saturation and fluid velocity change abruptly at this front. Liquid saturation passes from 1 behind the front to 0 in front of it, temperature jumps from the boiling temperature for the pressure existing at the front to the undisturbed reservoir temperature, and velocity is that of the injected liquid on one side and that of the vapor generated by its vaporization at the other.

Behind the front is a "hot liquid zone" where the liquid saturation is 1 and temperature is nearly constant. Still further behind, the temperature decreases to that of injected liquid. The hot liquid-cold liquid front is the classical "temperature front" of liquid saturated systems (Bodvarsson, 1972). In Fig. 1 this second front appears strongly smeared out by conduction and numerical dispersion.

Figure 2 shows typical variations with time of steam flow-rate, temperature of the liquid at the boiling front, and the volume of liquid water accumulated in the system. After an initial transient, production rate and boiling temperature tend to stabilize. The boiling temperature is always controlled by the pressure at the boiling front. As in our simulation the liquid-saturated interval remains small with respect to the total length

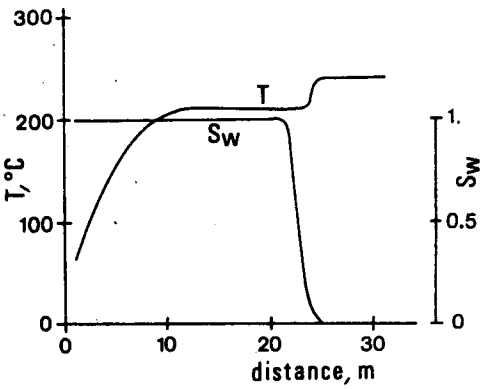

Fig. 1. One-dimensional, porous medium column. Temperature and saturation profiles for q_{inj} = 2.75e-3 kg/sm^2, k=5e-13 m^2.

Table I. Parameters used in one-dimensional models

Parameter	Problem		
	1-D linear porous	1-D linear fractured	1-D radial fractured
Length, m	300	300	
Cross sectional area, m^2	1	1	
Radius, m			300
Thickness, m			50
Initial temperature, °C	240	240	240
Initial pressure, bars	6	6	6
Const. pressure boundary, bars	6	6	6
Injection enthalpy, J/kg	125800	125800	125800
Injection rate, kg/s	6.3e-6 -2.34e-2	3.e-4	2.78
ROCKS			
Density, kg/m^3	2600	2600	2600
Porosity	8%	8%	8%
Heat conductivity, W/m °C	2.51	2.51	2.51
Specific heat, J/kg °C	920	920	920
Permeability, m^2	5e15 -1e-12	5e-18	5e-18
Relative permeability: (Corey curves)	S_{rw} =.30 S_{rv} = .05	S_{rw} =.30 S_{rv} = .05	S_{rw} =.30 S_{rv} = .05
FRACTURES			
Two vertical orthogonal sets spacing, m		25	25
Equivalent continuum porosity		1%	1%
Equivalent continuum permeability		5e-13	5e-13
Relative permeability:		liquid vapor	$k_{rw} = (S_w\text{-}0.01/0.99$ $k_{rv} = (0.99\text{-}S_w)/0.99$

of the column, boiling temperature and steam production remain almost constant during the simulation and the temperature in the hot liquid zone almost uniform. When injection starts and some of the injected water is vaporized, the pressure at the boiling front and the steam flow increase. As pressure (and temperature) at the boiling front increase, however, the heat released by the rock, and the boiling rate, decrease. Stabilization of temperature and steam flow-rate occur when the (increasing) steam flow equals the (decreasing) boiling rate.

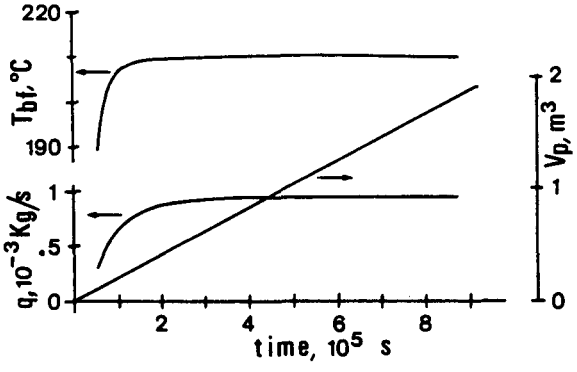

Fig. 2. One-dimensional, porous medium column. Production rate, boiling temperature and volume of liquid phase versus time for q_{inj} = 2.75e-3 kg/sm^2, k=5e-13 m^2.

The phenomena involved when stabilization of temperature and flow-rate are reached can be approximately described by a simple set of equations. Under the hypothesis that the heat released by the cooling rock equals the heat required for vaporization of liquid water, the heat balance for a column of unit cross section can be written as

$$v_{bf}(1-\phi)\rho_R C_R \Delta T = q_v h_{lv} \qquad (1)$$

The velocity of advancement of the boiling front is less than the velocity of liquid behind it, as a fraction of the liquid arriving at the front is vaporized. For a column of unit cross section we have

$$v_{bf} = \frac{q_{liq} - q_v}{\phi \rho_w} \qquad (2)$$

The steam flow in the dry steam zone is

$$q_v = k\frac{m_{bf} - m_c}{L} \qquad (3)$$

m being the pseudopressure at initial reservoir temperature. As q_{liq} is approximately equal to q_{inj}, and $p_{bf} = p_{sat}$ the system can be solved for q_v and ΔT. From this set of equations it follows that the boiling temperature depends on the group q_{inj} L/k, and the ratio q_v/q_{inj} depends on ΔT.

These relations are shown in Figures 3 and 4, where the results of several numerical simulations (with injection rates and permeabilities varying by several orders of magnitude) are compared with those of the above system of equations. Other parameters being equal, boiling temperature increases when q_{inj} increases, since a higher pressure at the boiling front is required to sustain a higher rate of steam flow. For the same reason, boiling temperature increases when permeability decreases, or the length of the steam flow path, L, increases.

The ratio of production to injection rate increases with the cooling undergone by the rock.

One-dimensional, fractured-porous medium models

The phenomena occurring when cold water is injected into a porous medium are largely controlled by the solid-fluid temperature equilibrium. In fractured media the heat transfer between the rock and the fluid flowing through the fractures occurs at a finite rate, which entails some differences in behavior compared to ideal porous media. The porous media thermal fronts are typically sharp whereas in fractured media they become very diffuse (Lauwerier, 1955).

Two simple reservoir models have been adopted to study the phenomenology of injection into fractured-porous media: a one-dimensional column and a one-dimensional radial system. In the first case cold water is injected at one end of the column and a constant pressure is maintained at the other end. In the second case water is injected at the center of the system and a constant pressure is maintained at the outer boundary.

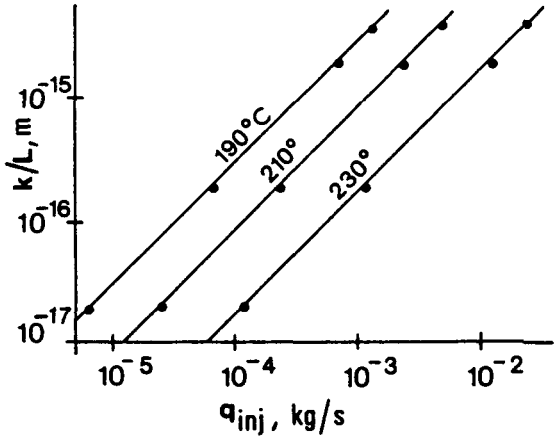

Fig. 3. One-dimensional, porous medium column. Dependence of stabilized boiling temperature on injection rate, permeability, and length of steam flow-path. Lines: from equations (1) to (3); solid circles: from numerical simulations.

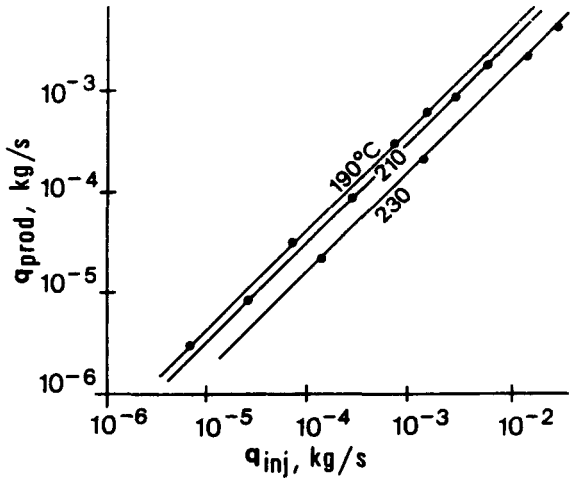

Fig. 4. One-dimensional, porous medium column. Dependence of q_{prod} on q_{inj} and boiling temperature. Lines: from equations (1) to (3); solid circles: from numerical simulations.

In both cases initial conditions are uniform temperature of 240 ° C and uniform pressure of 6 bars. The simulations have been performed using the method of "multiple interacting continua" (Pruess and Narasimhan, 1982, 1985). The parameters used for the simulations are shown in Table I.

Figure 5 shows a typical spatial distribution of temperature and saturation in the fractures for the one-dimensional column case. The liquid moves fast in the fractures and a wide two-phase zone is formed. Boiling takes place throughout the two-phase zone, at a rate which, at each point, depends essentially on the conductive heat flow from the matrix to the fractures. The hot liquid zone observed in the porous column is replaced, in this case, by an extended two-phase zone. The temperature is nearly uniform in the two-phase zone as it is controlled by the local pressure, which is nearly uniform due to the large fracture permeability. The temperature jumps abruptly to the initial reservoir temperature at the boundary between the two-phase and the dry zones. The temperature difference between the outermost elements of the matrix and the fractures is also shown in Fig. 5. This quantity is proportional

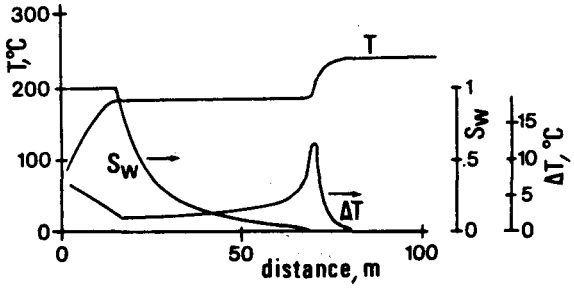

Fig. 5. One-dimensional, fractured medium column. Profiles of temperature and saturation in the fractures and temperature difference between outermost matrix elements and fractures for q_{inj} = 3e-4 kg/sm^2, k=5e-13 m^2

to the rate of matrix-fracture conductive heat flow, and reaches a maximum value at the leading edge of the two-phase zone.

The time evolution of some relevant quantities is shown in Figure 6. As in the porous column, boiling temperature and vapor production tend to stabilize after a short transient and temperature remains nearly uniform in the boiling zone (Fig. 6a). The flow rate of liquid entering the two-phase, boiling zone is slightly less than the injected water, as a fraction of the latter penetrates into the matrix (Fig 6b). This penetration is significant in the zone where the fractures are fully liquid-saturated, and is negligible in the two-phase zone. Both rates of liquid entering the matrix and the boiling zone tend to stabilize rapidly. The rate of vapor leaving the boiling zone also tends to stabilize to a lower value than the liquid inflow. The nearly constant difference between these two quantities causes the continuous widening of the boiling zone (Fig. 6). Due to this widening the distance between the boiling zone and the production boundary of the column is shortened considerably with a consequent slow decrease of the boiling temperature. It is interesting to observe that, while the boiling zone is spreading, the total heat flow from the matrix to the fractures in the boiling zone tends to stabilize. This means that the effect of decreasing heat flux from the matrix is compensated by an increase of the heat exchange surface. As in the porous column, the stabilization of temperature and flow rate occurs when the boiling rate equals the rate of vapor flow towards the production end.

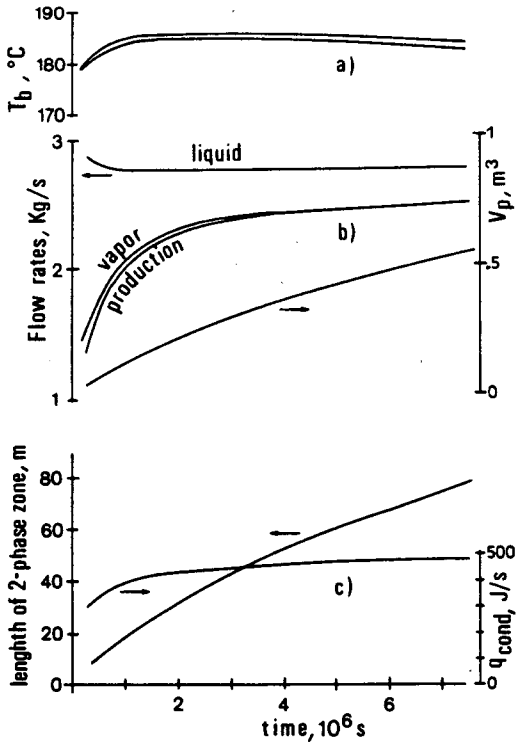

Fig. 6. One-dimensional column, fractured-porous medium. (a) Minimum and maximum temperature of two-phase fluid in the fractures. (b) Flow rates of liquid entering the two-phase zone in the fractures and flow of steam out of it; production rate at the constant pressure boundary; volume of liquid in the column (including the liquid fraction of the two-phase fluid). (c) Width of the zone with two-phase fluid in the fractures and total conductive matrix-fracture heat flow in this zone.

In the porous medium the velocity of the boiling front and the rock cooling adjust during the injection process so as to reach this condition. In the fractured medium, the rock-fluid heat transfer is limited and this condition is reached and maintained by enlargement of the boiling zone.

Figures 7 and 8 show results for the one-dimensional radial model. The only significant difference to the case with 1-D linear flow is that the width of the two-phase zone increases more slowly with time. In both cases the role of matrix blocks is essentially that of absorbing liquid from the fractures and releasing heat to them by conduction. The liquid inflow into the blocks becomes significant only when the surrounding fractures are fully liquid saturated. From this moment on, the liquid continues to flow into the block while the block is cooled by conduction. This process continues until the block is fully saturated with liquid at the temperature of the injected water.

TWO-DIMENSIONAL RADIAL, POROUS MEDIUM MODELS

Numerical experiments were also performed using more complex two-dimensional models, to obtain insight into fluid migration and phase transformation processes induced by injection on a reservoir scale, taking gravity into account. We consider a two-dimensional, radial porous medium system with a radius of 600 m (Fig. 9 and Table II). The injection well is placed at the center of the system and the production wells are assumed to be uniformly distributed in the region 150 m $<$ R $<$ 600 m. The reservoir is assumed to be 1000 m thick, with initial liquid saturation $S_w = 0$, and bounded below by a constant pressure surface with p = 64.1 bars and T = 280 ° C. All wells are assumed to have 50 m open intervals at the top of the reservoir. The production wells are placed on deliverability, with a bottom-hole pressure of 5 bars. Before starting injection, the system is run to steady-state heat conduction

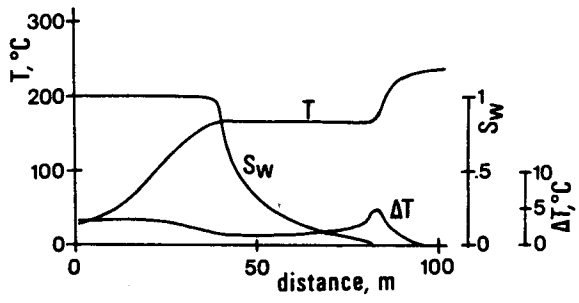

Fig. 7. One-dimensional radial, fractured-porous medium model (injection rate = 2.78 kg/s, k=5e-13 m^2). Variation with radial distance of temperature and liquid saturation in the fractures, and temperature difference between the outermost matrix elements and fractures.

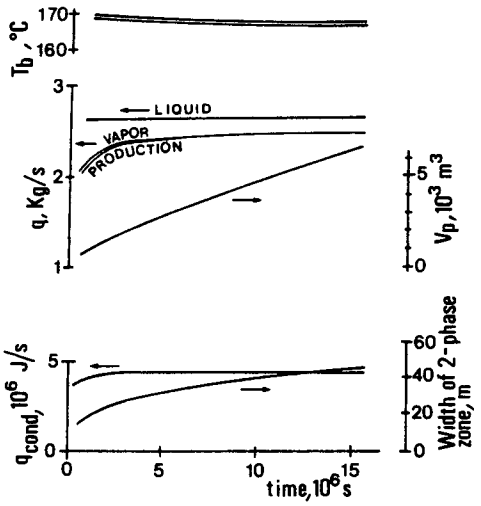

Fig. 8. One-dimensional radial, fractured-porous medium model. Temporal evolution of the same quantities as shown in Fig. 6.

(240 °C in the uppermost elements and 280 °C at the bottom) and quasi-steady mass flow at that temperature distribution. The production and recharge rates in this state are 58 kg/s, which is equal to the total pre-injection flow-rate of the wells at a distance of less than 600 m from the injection well for the field experiment reported by Giovannoni et al. (1981).

The simulations performed include three cases of injection into isotropic formations and one of anisotropic permeability, with vertical permeability one order of magnitude lower than horizontal. The permeability in zone c (see Table II) was adjusted so as to have the same initial production of the isotropic case. The parameters for the four cases are reported in Table II. The following general observations are made from the results obtained in all four cases (Figs. 10, 11, 12):

(1) The injection plume tends to move primarily downward from the injection well rather than laterally outward;

(2) most of the plume is in single-phase liquid conditions, with boiling restricted to the outer "skin" of the plume; (If the fractured-porous nature of the reservoir were taken into account we would expect more extensive two-phase zones.)

Table II. Parameters used in two-dimensional models

Parameter	Case 1	Case 2	Case 3	Case 4
Injection rate, kg/s	5	27.8	55.6	27.8
Injection enthalpy, J/kg	125800	125800	125800	125800
Wells on deliverability:				
productivity index per unit area, m^3/m^2	1.81e-15	1.81e-15	1.81e-15	1.81e-15
bottomhole pressure, bars	5	5	5	5
Initial liquid saturation	0	0	0	0
Specific heat, J/kg °C	920	920	920	920
Relative permeability: (Corey curves)	S_{rw}=.30 S_{rv}=.05	S_{rw}=.30 S_{rv}=.05	S_{rw}=.30 S_{rv}=.05	S_{rw}=.30 S_{rv}=.05
ZONE A				
Density, kg/m^3	2600	2600	2600	2600
Porosity	8%	8%	8%	8%
Heat conductivity, W/m °C	2.51	2.51	2.51	2.51
Horizontal permeability, m^2	5e-13	5e-13	5e-13	5e-13
Vertical permeability, m^2	5e-13	5e-13	5e-13	5e-14
ZONE B				
Density, kg/m^3	2700	2700	2700	2700
Porosity	5%	5%	5%	5%
Heat conductivity, W/m °C	2.87	2.87	2.87	2.87
Horizontal permeability, m^2	5e-13	5e-13	5e-13	5e-13
Vertical permeability, m^2	5e-13	5e-13	5e-13	5e-14
ZONE C				
Density, kg/m^3	2700	2700	2700	2700
Porosity	1%	1%	1%	1%
Heat conductivity, W/m °C	2.93	2.93	2.93	2.93
Permeability, m^2	4.5e-14	4.5e-15	4.5e-15	5.1e-15

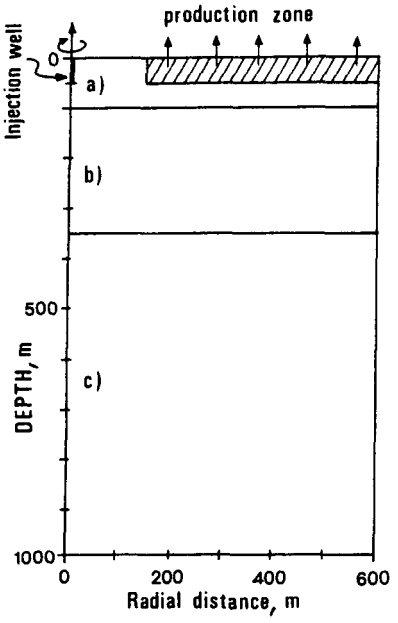

Fig. 9. Two-dimensional radial, porous medium model.

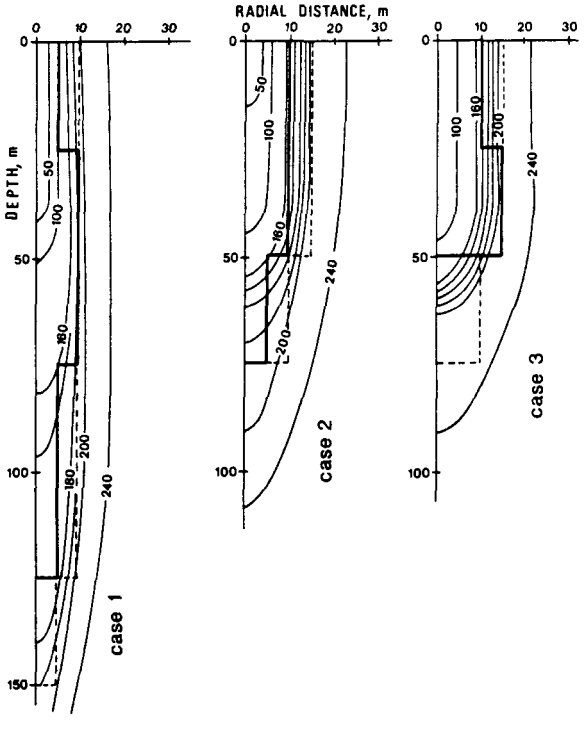

Fig. 10. Two-dimensional radial, isotropic porous medium model. Shape of the injection plume and isotherms for different injection rates. In all three cases the liquid volume (including the liquid in the two-phase elements) is about 2800 m^3. Continuous line: limit of liquid-saturated region. Dashed line: limit of two-phase region.

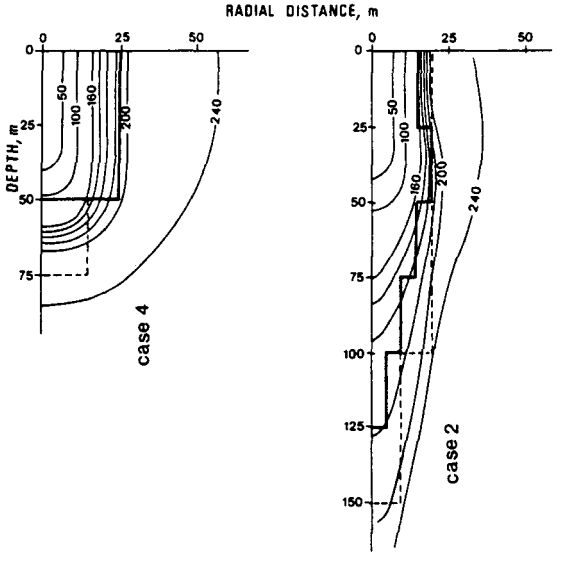

Fig. 11. Shape of the liquid plume and isotherms for the anisotropic and isotropic cases after approximately three weeks of injection, when liquid volume (including that in the two-phase elements) is about 8500 m^3. Continuous line: limit of liquid-saturated region. Dashed line: limit of two-phase region.

(3) after an initial transient, boiling temperatures again tend to stabilize and the temperature differences between different parts of the outer surface of the plume are limited to a few tens of degrees.

Once injection starts, the plume expands both downward and laterally. The shape assumed by the plume during its evolution depends on the relative importance of pressure and gravity forces. The lateral expansion is more pronounced for higher injection rate (Fig. 10). As the plume continues to expand, both its horizontal cross-section and the height of the liquid column increase, thus facilitating the downward movement of liquid water and decreasing the pressure in the upper parts of the plume. With time the lateral expansion of the plume slows down and eventually terminates. Other conditions being equal, the horizontal cross section reached is higher for higher injection rates. When the plume reaches the permeability discontinuity at 350 m depth below reservoir top, its downward propagation slows down considerably, and liquid migration occurs radially outward above the discontinuity surface. The liquid can propagate to below the producing area, but a thick layer of steam saturated, high temperature rock still separates the liquid-invaded reservoir volume from the shallow producing wells (Fig. 12). The boiling temperature is still controlled by the pressure in the boiling zone and tends to stabilize when boiling rate equals the steam flow towards the producing zone. In a two-dimensional system the spatial distribution of boiling temperature depends on the steam flow pattern. Boiling temperature is higher for higher injection rates (Fig. 10), as higher pressure in the boiling zone is needed to maintain a higher rate of steam flow. Boiling temperature also increases with depth due to the

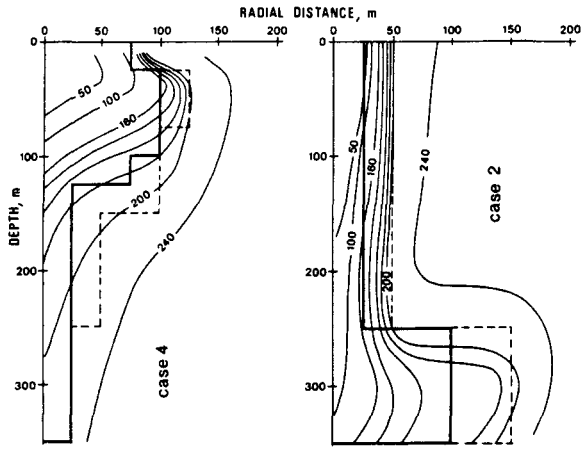

Fig. 12. Shape of the liquid plume and isotherms for the anisotropic and isotropic cases after approximately one year of injection, when liquid volume (including that in the two-phase elements) is about 356,000 m^3. Continuous line: limit of liquid-saturated region. Dashed line: limit of two-phase region.

higher initial reservoir temperature, and the greater distance from the producing zone. Due to the high permeability assumed in our models in the upper part of the reservoir, these differences remain limited.

After the lateral expansion of the plume has stopped, the temperature inside the plume continues to decrease due to flow of cold injected water. The temperature of the stationary (at shallower depth) skin of the plume would also tend to decline. However, this process can not go very far because of the coupling between temperature and pressure in a two-phase system. In response to very small temperature-and-pressure declines at the lateral boundary of the plume the vaporization process terminates there. Subsequently vapor flows towards the shallow surface of the plume, where it condenses, depositing its latent heat. The "skin" of the plume is still kept at a high temperature by steam condensation and conductive heat flow. In such conditions, the downflow of liquid inside the plume is larger than the injection flowrate.

Figures 11 and 12 compare the plumes for cases 2 and 4 (anisotropic) at different stages of evolution. Figure 11 shows the shape of the plume and the isotherms in an early stage of its evolution. In both cases the lateral expansion of the plume is still underway. Although the coarse mesh used was inadequate for a detailed analysis of the long time behavior of the systems, Fig. 12 nevertheless reveals some significant differences between the two cases and illustrates some of the above-described phenomena. After about one year of injection, in the anisotropic case, the bottom of the plume has only just reached the permeability discontinuity. The plume still continues to expand laterally, and the two-phase zone has advanced to near the production zone. In case 2 the lateral expansion of the upper parts of the plume has already ended and the horizontal movement of the plume above the permeability discontinuity surface is evident. Figure 13 shows the pressure distribution in the dry steam zone for case 2 at the same time as Fig. 12. The pressure distribution clearly shows the flow of steam from the deep boiling zones to the upper condensing zones of the plume "skin".

CONCLUSIONS

Injection of cold water into depleted vapor zones gives rise to complex coupled processes of fluid flow and heat transfer. Temperature and phase fronts tend to be sharp in porous medium models, but become very diffuse in fractured media, where the thermal equilibration between fluids in the fractures and reservoir rock is delayed. The following observations were made in our numerical experiments.

(1) After an initial transient, boiling temperature at the surface of the injection plume tends to stabilize.

(2) Stabilized boiling temperature depends primarily on injection rate and reservoir permeability, being larger for larger rate and smaller permability.

(3) When gravity effects are included the injection plume tends to move primarily downward from the injection point rather than laterally outward.

(4) Vaporization and condensation processes tend to keep temperature variations limited over the entire surface of the plume.

In summary, it appears that a number of fluid flow and heat transfer processes combine to make cold water injection into depleted vapor zones an efficient heat extraction process.

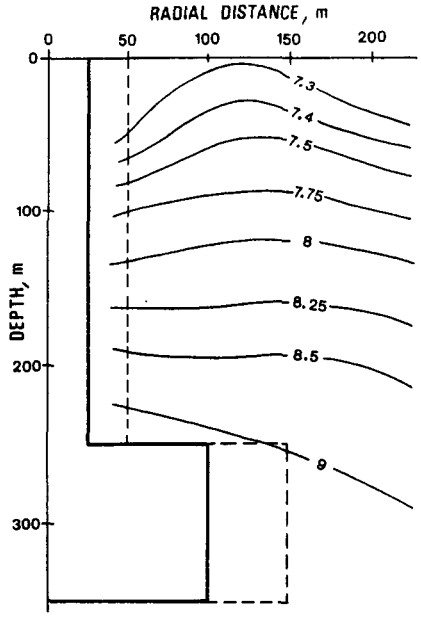

Fig. 13. Pressure distribution (bars) around the "plume" for case 2.

NOMENCLATURE

c_r	specific heat of rock, J/kg °C
h_{lv}	latent heat of vaporization, J/kg
k	permeability, m^2
L	distance of boiling front from the constant pressure boundary, m
m	pseudopressure, Pa s/m^2
p	pressure, Pa
p_{sat}	saturation pressure, Pa
q	flux, kg/s·m^2
q_{cond}	total conductive heat flow, J/s
q_{inj}	injection flux, kg/s·m^2
q_{liq}	flux of liquid behind the boiling front, kg/s·m^2
q_{prod}	production flux, kg/s·m^2
q_v	steam flux, kg/s·m^2
R	radius, m
S	saturation, dimensionless
S_{rw}	irreducible liquid saturation, dimensionless
S_{rv}	irreducible vapor saturation, dimensionless
T	temperature, °C
v_{bf}	boiling front velocity, m/s
V_w	volume of liquid in the system, including that in the 2-phase fluid, m^3
ϕ	porosity, dimensionless
ρ	density, kg/m^3

Subscripts

b	boiling zone
bf	boiling front
c	constant pressure boundary
r	rock
v	vapor
w	liquid

ACKNOWLEDGEMENT

This work was supported by the Progetto Strategico Valorizzazione Materie Prime Minerali, CNR, Italy, and by the U.S. Department of Energy, Geothermal Technology Division, under Contract No. DE-AC03-76SF00098. For assistance in the preparation of the manuscript, the authors are indebted to M. H. Dickson, G. Gori, E. Klahn, L. Fairbanks, and M. Bodvarsson.

REFERENCES

Bertrami, R., Calore, C., Cappetti, G., Celati, R., D'Amore, F., 1985, A three-year recharge test by reinjection in the general area of Larderello field: analysis of production data. 1985 International Symp. on Geothermal Energy, Kailua-Kona, Hawaii, Vol. 9, pt. 2, pp. 293-298.

Bodvarsson, G., 1972, Thermal problems in the siting of reinjection wells, *Geothermics,* Vol. 1, No. 1, pp. 63-68.

Cappetti, G., Giovannoni, A., Ruffilli, C., Calore, C., Celati, R., 1982, Reinjection in the Larderello geothermal field, Proceedings International Conference on Geothermal Energy, Firenze, BHRA Fluid Engineering, Cranfield, Bedford (England), pp. 395-408.

Giovannoni, A., Allegrini, R., Cappetti, G., Celati, R., 1981, First results of a reinjection experiment at Larderello, Proceedings of 7th Workshop Geothermal Reservoir Engineering, Stanford, California, pp. 77-84.

Lauwerier, H. A., 1955, The transport of heat in an oil layer caused by the injection of hot fluid, Appl. Sci. Res., Martinus Nijhoff, Publisher, The Hague, Vol. 5, Section A, No. 2-3, pp. 145-150.

Pruess, K., 1983, Development of the general purpose simulator MULKOM, Annual Report 1982, Earth Science Division, Report LBL-15500, Lawrence Berkeley Laboratory.

Pruess, K. and Narasimhan, T. N., 1982, On fluid reserves and the production of superheated steam from fractured, vapor-dominated geothermal reservoirs, *Journal of Geophysical Research,* Vol. 87, No. B11, pp. 9329-9339.

Pruess, K. and Narasimhan, T. N., 1985, A practical method for modeling fluid and heat flow in fractured porous media, *SPE Journal,* February, pp. 14-26.